

Template-Free Synthesis of a Highly Porous Benzimidazole-Linked Polymer for CO₂ Capture and H₂ Storage

Mohammad G. Rabbani and Hani M. El-Kaderi*

Department of Chemistry, Virginia Commonwealth University, Richmond, Virginia 23284-2006, United States

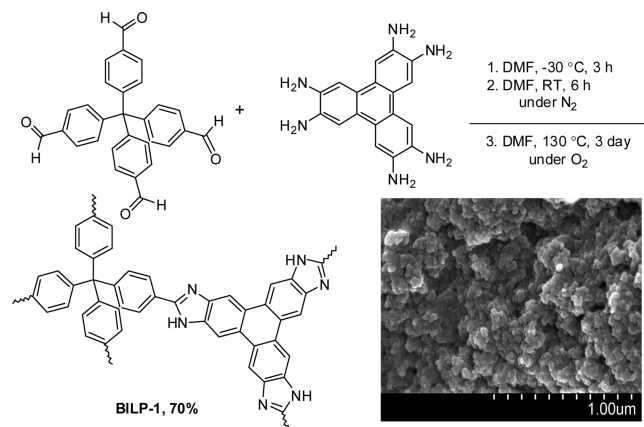
Supporting Information

KEYWORDS: polybenzimidazole, porous polymers, carbon dioxide capture, hydrogen storage, gas separation

The design and synthesis of highly porous organic polymers has attracted considerable attention due to their potential use in gas storage and separation, catalysis, electronics, and chemical sensing.¹ Among these polymers are polybenzimidazoles (PBIs) which have been mainly investigated as membranes in proton-exchange membrane fuel cells (PEMFCs) application.² PBIs are usually prepared by polycondensation reactions between aryl-*o*-diamines and benzene carboxylic acids in the presence of templating agents such as silica nanoparticles or porogen in polyphosphoric acid; other methods also include ionothermal and melt-condensation routes.³ The resulting polymers possess surface areas up to ~ 200 m²/g and pore sizes in the macroporous to microporous ranges. In spite of the great research efforts in this field, the surface area of PBIs remains considerably lower than those observed for purely organic polymers such as polymers of intrinsic microporosity (PIMs),⁴ porous aromatic frameworks (PAFs),⁵ covalent organic frameworks (COFs),⁶ and porous polymer networks (PPNs).⁷ The functional nature of PBIs stems from the amphoteric imidazole moieties which are part of the polymer backbone, and consequently, PBIs are attractive for gas storage and separation studies. For example, introducing amine functionality or accessible nitrogen sites into the pore wall of metal organic frameworks (MOFs),⁸ zeolitic imidazolate frameworks (ZIFs),⁹ or zeolitic tetrazolate frameworks (ZTFs)¹⁰ can drastically impact their gas uptake and selectivity. In particular, the selective uptake of CO₂ over CH₄ or N₂ is believed to arise from enhanced CO₂–framework interactions through hydrogen bonding and/or dipole–quadrupole interactions.¹¹ CO₂ is a green house gas which contributes significantly to global warming, hence developing highly efficient materials for its sequestration or separation from natural gas or flue gases will have a direct environmental and economical impact.¹²

With these considerations in mind, we report herein on template-free synthesis of a highly porous benzimidazole-linked polymer (BILP-1) by the condensation reaction between 2,3,6,7,10,11-hexaaminotriphenylene (HATP) and tetrakis(4-formylphenyl)methane (TFPM) (Scheme 1). The resulting polymer was characterized by spectral and analytical methods, while porosity was investigated by argon sorption measurement. A dropwise treatment of a suspension of HATP in *N,N*-dimethylformamide (DMF) with homogeneous solution of TFPM in DMF over 3 h at -30 °C followed by stirring at room temperature for 6 h afforded a yellow suspension (presumably imine-

linked oligomers).^{13,14} The resulting suspension was bubbled with oxygen and then heated in a sealed Schlenk flask at 130 °C for 3 days to afford BILP-1 (70%) as a yellow powder after filtration and drying at 120 °C and 1.0×10^{-5} Torr for 12 h. The slow addition of TFPM and the use of DMF increase initial oligomer solubility and prevent their premature precipitation which enhances pore formation and, therefore, the overall porosity.¹⁴ The formation of the imidazole ring proceeds through a rapid formation of imine-linkage followed by cyclization assisted by molecular oxygen.¹³

Scheme 1. Synthesis of BILP-1 and Scanning Electron Microscopy (SEM) Image of the As-Prepared Polymer (inset)

BILP-1 is insoluble in water and common organic solvents such as hexane, methanol, acetone, tetrahydrofuran, and DMF. Storing the material under aerobic conditions for one month or treatment with a 2 M solution of HCl or NaOH lead only to a slight color change from yellow to brown presumably due to the oxidation of unreacted terminal amino groups on the surface of the polymer particles. The chemical composition was determined by elemental analysis¹⁵ which showed that the Lewis basic sites involve in hydrogen bonding with about one water molecule per site. A similar observation has been reported for the imine-linked COF-300.^{6c}

Received: February 8, 2011**Revised:** March 10, 2011**Published:** March 16, 2011

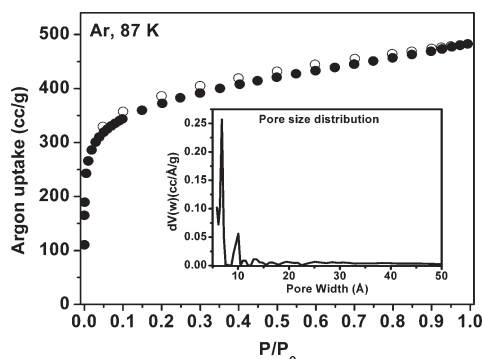


Figure 1. Argon uptake isotherm at 87 K; adsorption (filled) and desorption (empty). Inset NLDFT pore size distribution.

This was further supported by thermogravimetric analysis (TGA) which showed weight loss between 50 to 100 °C that corresponds to the removal of water molecules followed by decomposition at ~400 °C (Supporting Information, S1). Scanning electron microscopy (SEM) established phase purity of the polymer and revealed aggregated particles ~100–300 nm in size (Scheme 1, inset). The material is amorphous as evidenced by powder X-ray diffraction analysis (Supporting Information, S3). The chemical connectivity and the formation of the imidazole ring were confirmed by FT-IR and ^{13}C solid-state NMR spectroscopy. The FT-IR spectrum of BILP-1 (Supporting Information, S4–5) showed N—H stretching at 3417 (free N—H) and 3185 cm^{-1} (hydrogen bonded N—H), a characteristic feature of polybenzimidazole NH absorptions.^{16a,b} A new intense band appeared at 1482 cm^{-1} which corresponds to C=N stretching of the benzimidazole ring.^{16c,d} The broad band at around 1625 cm^{-1} is presumably due to the overlap of C=C and C=N stretching bands. In addition, the absence of a C=O stretching band at 1702 cm^{-1} indicates a full consumption of the TFPM monomer. The imidazole ring formation and the incorporation of intact triphenylene or tetraphenylmethane units into the polymer network was examined by ^{13}C CP-MAS NMR measurement. The NMR spectrum (Supporting Information, S9) contains a signal at 151 ppm which corresponds to the NC(Ph)N in benzimidazole units. This is in sharp contrast to the reported signals for Ph—C=N—Ph in imine-linked frameworks such as COF-300,^{6c} polymer organic frameworks (POFs), and^{14a} poly(azomethine) networks (ANW),^{14b} which appear at 160–158 ppm. Additional signals in the aromatic range support the incorporation of intact tetraphenylmethane and triphenylene units into the network.

In contrast to COF-300 which decomposes readily upon treatment with 2 M HCl due to cleavage of the acid sensitive imine-linkage, BILP-1 remains intact in 2 M HCl as a result of the more chemically robust imidazole ring. Given the physical rigidity and dimensionality of the building units employed in the construction of BILP-1 which are analogous to the building blocks in COF-105 and COF-108,^{6a} we anticipated BILP-1 to be highly porous. Therefore, it was of interest to us to subject the material to porosity studies and to evaluate its performance in the storage of small gases and separation.

The porous nature of the polymer was evaluated by argon uptake measurements at 87 K and 1 bar. The fully reversible isotherm depicted in Figure 1 shows a rapid uptake at low pressure (0–0.1 bar) indicating a permanent microporous nature. The gradual increase in argon uptake and the minor hysteresis may be due to the flexible nature of organic polymers. Applying the

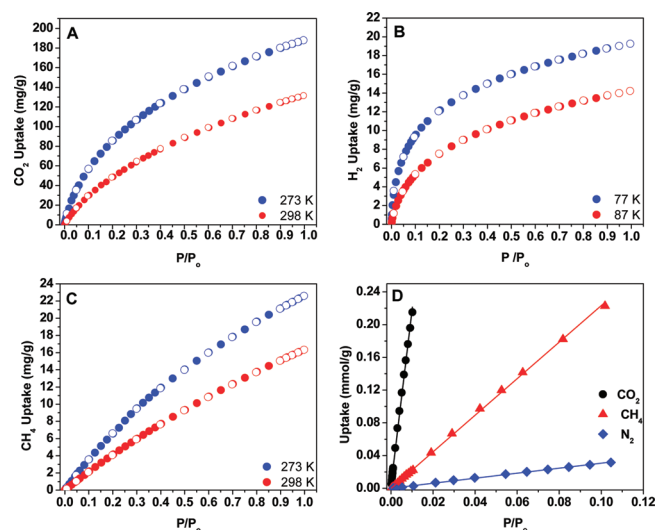


Figure 2. Gas uptake isotherms CO_2 (A), H_2 (B), and CH_4 (C); adsorption (filled) and desorption (empty). Initial gas uptake slopes at 273 K (D).

Brunauer–Emmett–Teller (BET) model within the pressure range of $P/P_0 = 0.05$ – 0.15 resulted in an apparent surface area of 1172 $\text{m}^2 \text{g}^{-1}$ which makes BILP-1 the most porous purely organic benzimidazole-linked polymer reported to date.^{2a} This surface area is comparable to the reported values for 3-D crystalline imine-linked COF-300 (1360 $\text{m}^2 \text{g}^{-1}$),^{6c} POFs (466–1521 $\text{m}^2 \text{g}^{-1}$),^{14a} and diimide-based polymers (750–1407 $\text{m}^2 \text{g}^{-1}$).¹⁷ Pore size distribution was examined by fitting the uptake branch of the argon isotherm with nonlocal density functional theory (NLDFT) and was found to be centered at 6.8 Å (Figure 1, inset), while the total pore volume calculated at $P/P_0 = 0.95$ is 0.70 $\text{cm}^3 \text{g}^{-1}$.

To investigate the impact of microporosity and the amphoteric pore walls of BILP-1 on the uptake of small gases and selectivity, we collected CO_2 , CH_4 , and H_2 isotherms and calculated their respective isosteric enthalpies of adsorption (Q_{st}). CO_2 isotherms were measured at 273 and 298 K from 0 to 1 bar (Figure 2A). The isotherms are fully reversible and exhibit a steep rise at low pressures then reach 188 and 131 mg/g at 273 and 298 K, respectively. The Q_{st} for CO_2 was estimated from adsorption data collected under these conditions using the virial method.¹⁸ At zero coverage, the Q_{st} is 26.5 kJ/mol and drops to 19.7 kJ/mol as the uptake reaches 188 mg/g (Supporting Information, S17). The CO_2 uptake and Q_{st} are higher than the values reported for COFs,¹⁹ imine-lined organic cages,²⁰ or diimide polymers^{17b} and comparable to CO_2 selective MOFs⁸ or ZTF¹⁰ which generally feature $-\text{NH}_2$ or $-\text{OH}$ functionalized pores. The relatively high CO_2 uptake and binding by BILP-1 are most likely due to favorable interactions of the polarizable CO_2 molecules through hydrogen bonding and/or dipole–quadrupole interactions that utilize the protonated- and proton-free nitrogen sites of imidazole rings, respectively.^{10,12} The readily reversible sorption/desorption behavior indicates that CO_2 interactions with pore walls are weak enough to allow for material regeneration without applying heat. This is attractive because materials that have strong acidic or basic sites usually display high CO_2 affinities and require energy input (in the form of heat) to regenerate their active sites as in the case of primary alkanolamine MEA.²¹ This drawback remains one of the great challenges in current CO_2 capture technologies.

In addition to CO₂ capture and separation by porous materials, extensive studies on hydrogen and methane storage have been reported because of their potential in automotive applications.²² The hydrogen isotherms depicted in Figure 2B are fully reversible and the uptake reaches 19 and 14 mg/g at 77 and 87 K, respectively. The Q_{st} for H₂ was calculated from adsorption data collected at 77 and 87 K. At zero-coverage, the Q_{st} is 7.9 kJ/mol which shows a gradual drop as more hydrogen gets adsorbed and reaches 5.8 kJ/mol at 1.9 wt % loading (Supporting Information, S18). The Q_{st} value is higher than the values reported for organic polymers such as of COFs (6.0–7.0 kJ/mol),¹⁹ PAF-1 (4.6 kJ/mol),⁵ polyimide networks (5.3–7.0 kJ/mol),^{17a} and PPNs (5.5–7.6 kJ/mol).⁷ Similarly, we recorded CH₄ uptake at 273 and 298 K up to 1 bar (Figure 2C). Again, both isotherms are completely reversible and exhibit a steep rise at low pressure and then reach maxima of 23 and 16 mg/g at 273 and 298 K, respectively. The Q_{st} for CH₄ was calculated by using adsorption data collected at 273 and 298 K. At zero coverage, the Q_{st} is 16.3 kJ/mol which drops to 10.0 kJ/mol at 23.0 mg/g loading (Supporting Information, S19). A noticeable lower Q_{st} value of CH₄ compared to that of CO₂ is due to the nonpolar nature of methane. We have also considered the selective uptake of small gases (CO₂, CH₄, N₂) to evaluate the potential use of BILP-1 in gas separation applications. The selectivity of BILP-1 toward CO₂ over N₂ and CH₄ was investigated by collecting isotherms at 273 and 298 K (Supporting Information, S20). At 273 K and 0.1 bar, which is a typical partial pressure of CO₂ in flue gases, the CO₂ uptake is 1.28 mmol/g whereas that of N₂ is only 0.03 mmol/g. On the basis of initial slope calculations in the pressure range of 0 to 0.1 bar, the estimated adsorption selectivity for CO₂ over N₂ is 70 (Figure 2D). This selectivity surpasses carbon-based materials²³ or ZIFs⁹ and is comparable to Bio-MOF-11 (81)^{8a} and non-covalent porous materials (NPMs) (74).²⁴ Furthermore, the CO₂ selectivity of BILP-1 over CH₄ was calculated using initial slopes calculations (10 at 273 K and 7 at 298 K). Again, these values exceed those reported for activated carbon and ZIFs, as well as that of the recently reported diimide polymer. The high selectivity of CO₂ over N₂ and CH₄ stems from the fact that under the above-mentioned conditions, the imidazole moieties of BILP-1 interact more favorably with the polarizable CO₂ molecules through hydrogen bonding and/or dipole–quadrupole interactions involving the protonated- and proton-free nitrogen sites, respectively.

In conclusion, we have proved that a simple template-free condensation reaction between 2,3,6,7,10,11-hexaaminotriphenylene and tetrakis(4-formylphenyl)methane affords a highly porous benzimidazole-linked polymer which exhibits a promising potential in gas storage and separation applications. The high chemical stability and surface area of BILP-1 make it attractive for postsynthesis nanoimpregnation with acids for use in proton-exchange membrane fuel cells (PEMFCs) or to enhance selective gas uptake. These aspects are currently being addressed in our laboratory.

■ ASSOCIATED CONTENT

S Supporting Information. Experimental procedures, characterization methods, and gas sorption and separation studies (PDF). This material is available free of charge via the Internet at <http://pubs.acs.org>.

■ AUTHOR INFORMATION

Corresponding Author

*E-mail: helkaderi@vcu.edu. Tel: (804) 828-7505. Fax: (804) 828-8599.

■ ACKNOWLEDGMENT

We are grateful to the U.S. Department of Energy, Office of Basic Energy Sciences (DE-SC0002576) for generous support of this project. H.M.E. acknowledges support of the Donors of the American Chemical Society Petroleum Research Fund ACS-PRF (48672-G5). We thank T.E. Reich for his help with heat of adsorption calculations.

■ REFERENCES

- (1) (a) McKeown, N. B.; Budd, P. M. *Macromolecules* **2010**, *43*, 5163–5176. (b) McKeown, N. B.; Budd, P. M. *Chem. Soc. Rev.* **2006**, *35*, 675–683. (c) Thomas, A.; Kuhn, P.; Weber, J.; Titirici, M.-M.; Antonietti, M. *Macromol. Rapid Commun.* **2009**, *30*, 221–236.
- (2) (a) Asensio, J. A.; Sánchez, E. M.; Gómez-Romero, P. *Chem. Soc. Rev.* **2010**, *39*, 3210–3239. (b) Weber, J.; Kreuer, K.-D.; Maier, J.; Thomas, A. *Adv. Mater.* **2008**, *20*, 2595–2598.
- (3) (a) Weber, J.; Antonietti, M.; Thomas, A. *Macromolecules* **2007**, *40*, 1299–1304. (b) Mecerreyes, D.; Grande, H.; Miguel, O.; Ochoteco, E.; Marcilla, R.; Cantero, I. *Chem. Mater.* **2004**, *16*, 604–607. (c) Weber, J. *ChemSusChem* **2010**, *3*, 181–187. (d) Graberg, T. V.; Thomas, A.; Greiner, A.; Antonietti, M.; Weber, J. *Macromol. Mater. Eng.* **2008**, *293*, 815–819.
- (4) (a) Ghanem, B. S.; Hashem, M.; Harris, K. D. M.; Msayib, K. J.; Xu, M.; Budd, P. M.; Chaukura, N.; Book, D.; Tedds, S.; Walton, A.; McKeown, N. B. *Macromolecules* **2010**, *43*, 5287–5294. (b) Du, N.; Robertson, G. P.; Pinnau, I.; Guiver, M. D. *Macromolecules* **2010**, *43*, 8580–8587.
- (5) Ben, T.; Ren, H.; Ma, S. Q.; Cao, D. P.; Lan, J. H.; Jing, X. F.; Wang, W. C.; Xu, J.; Deng, F.; Simmons, J. M.; Qiu, S. L.; Zhu, G. S. *Angew. Chem., Int. Ed.* **2009**, *48*, 9457–9460.
- (6) For selected papers on COFs, please see: (a) El-Kaderi, H. M.; Hunt, J. R.; Mendoza-Cortés, J. L.; Côté, A. P.; Taylor, R. E.; O’Keeffe, M.; Yaghi, O. M. *Science* **2007**, *316*, 268–272. (b) Côté, A. P.; Benin, A. I.; Ockwig, N. W.; O’Keeffe, M.; Matzger, A. J.; Yaghi, O. M. *Science* **2005**, *310*, 1166–1170. (c) Uribe-Romo, F. J.; Hunt, J. R.; Furukawa, H.; Klöck, C.; O’Keeffe, M.; Yaghi, O. M. *J. Am. Chem. Soc.* **2009**, *131*, 4570–4571. (d) Côté, A. P.; El-Kaderi, H. M.; Furukawa, H.; Hunt, J. R.; Yaghi, O. M. *J. Am. Chem. Soc.* **2007**, *129*, 12914–12915. (e) Hunt, J. R.; Doonan, C. J.; LeVangie, J. D.; Côté, A. P.; Yaghi, O. M. *J. Am. Chem. Soc.* **2008**, *130*, 11872–11873.
- (7) Lu, W.; Yuan, D.; Zhao, D.; Schilling, C. I.; Plietzsch, O.; Muller, T.; Bräse, S.; Guenther, J.; Blümel, J.; Krishna, R.; Li, Z.; Zhou, H.-C. *Chem. Mater.* **2010**, *22*, 5964–5972.
- (8) (a) An, J.; Geib, S. J.; Rosi, N. L. *J. Am. Chem. Soc.* **2010**, *132*, 38–39. (b) Demessence, A.; D’Alessandro, D. M.; Foo, M. L.; Long, J. R. *J. Am. Chem. Soc.* **2009**, *131*, 8784–8786. (c) Arstad, B.; Fjellvåg, H.; Kongshaug, K. O.; Swang, O.; Blom, R. *Adsorption* **2008**, *14*, 755–762. (d) Vaidhyanathan, R.; Iremonger, S. S.; Dawson, K. W.; Shimizu, G. K. H. *Chem. Commun.* **2009**, 5230–5232. (e) Vaidhyanathan, R.; Iremonger, S. S.; Shimizu, G. H. K.; Boyd, P. G.; Alavi, S.; Woo, T. K. *Science* **2010**, *330*, 650–653.
- (9) (a) Phan, A.; Doonan, C. J.; Uriberomo, F. J.; Knobler, C. B.; O’Keeffe, M.; Yaghi, O. M. *Acc. Chem. Res.* **2010**, *43*, 58–67. (b) Wang, B.; Côté, A. P.; Furukawa, H.; O’Keeffe, M.; Yaghi, O. M. *Nature* **2008**, *453*, 207–212.
- (10) Panda, T.; Pachfule, P.; Chen, Y.; Jiang, J.; Banerjee, R. *Chem. Commun.* **2011**, *47*, 2011–2013.
- (11) Zheng, B.; Bai, J.; Duan, J.; Wojtas, L.; Zaworotko, M. J. *J. Am. Chem. Soc.* **2011**, *133*, 748–751.

- (12) (a) D'Alessandro, D. M.; Smit, B.; Long, J. R. *Angew. Chem., Int. Ed.* **2010**, *49*, 2–27. (b) Ma, S. Q.; Zhou, H. C. *Chem. Commun.* **2010**, *46*, 44–53. (c) Keskin, S.; van Heest, T. M.; Sholl, D. S. *ChemSusChem* **2010**, *3*, 879–891.
- (13) (a) Neuse, E. W.; Loonat, M. S. *Macromolecules* **1983**, *16*, 128–136. (b) Lin, S.; Yang, L. *Tetrahedron Lett.* **2005**, *46*, 4315–4319.
- (14) (a) Pandey, P.; Katsoulidis, A. P.; Eryazici, I.; Wu, Y.; Kanatzidis, M. G.; Nguyen, S. T. *Chem. Mater.* **2010**, *22*, 4974–4979. (b) Schwab, M. G.; Hamburger, M.; Feng, X.; Shu, J.; Spiess, H. W.; Wang, X.; Antonietti, M.; Müllen, K. *Chem. Commun.* **2010**, *46*, 8932–8934.
- (15) Elemental analysis for $C_{159}H_{84}N_{24} \cdot 12H_2O$. Calculated: C, 74.99; H, 4.27; N, 13.20%. Found: C, 73.81; H, 4.97; N, 12.65%.
- (16) (a) Bouchet, R.; Siebert, E. *Solid State Ionics* **1999**, *118*, 287–299. (b) Feng, S.; Shang, Y.; Wang, S.; Xie, X.; Wang, Y.; Wang, Y.; Xu, J. *J. Membr. Sci.* **2010**, *346*, 105–112. (c) Schoone, K.; Smets, J.; Houben, L.; Van Bael, M. K.; Adamowicz, L.; Maes, G. J. *Phys. Chem. A* **1998**, *102*, 4863–4877. (d) Morsy, M. A.; Al-Khaldi, M. A.; Suwaiyan, A. J. *Phys. Chem. A* **2002**, *106*, 9196–9203.
- (17) (a) Wang, Z.; Zhang, B.; Yu, H.; Sun, L.; Jiaob, C.; Liua, W. *Chem. Commun.* **2010**, *46*, 7730–7732. (b) Farha, O. K.; Spokoyny, A.; Hauser, B.; Bae, Y.-S.; Brown, S.; Snurr, R. Q.; Mirkin, C. A.; Hupp, J. T. *Chem. Mater.* **2009**, *21*, 3033–3035.
- (18) (a) Rowsell, J. L. C.; Yaghi, O. M. *J. Am. Chem. Soc.* **2006**, *128*, 1304–1315. (b) Britt, D.; Furukawa, H.; Wang, B.; Glover, T. G.; Yaghi, O. M. *Proc. Natl. Acad. Sci. U.S.A.* **2009**, *106*, 20637–20640.
- (19) Furukawa, H.; Yaghi, O. M. *J. Am. Chem. Soc.* **2009**, *131*, 8875–8883.
- (20) Tozawa, T.; Jones, J. T. A.; Swamy, S. I.; Jiang, S.; Adams, D. J.; Shakespeare, S.; Clowes, R.; Bradshaw, D.; Hasell, T.; Chong, S. Y.; Tang, C.; Thompson, S.; Parker, J.; Trewin, A.; Bacsa, J.; Slawin, A. M. Z.; Steiner, A.; Cooper, A. I. *Nat. Mater.* **2009**, *8*, 973–978.
- (21) Rochelle, G. T. *Science* **2009**, *325*, 1652–1654.
- (22) Li, J.-R.; Kuppler, R. J.; Zhou, H.-C. *Chem. Soc. Rev.* **2009**, *38*, 1477–1504.
- (23) Cavenati, S.; Grande, C. A.; Rodrigues, A. E. *J. Chem. Eng. Data* **2004**, *49*, 1095–1101.
- (24) Lewiński, J.; Kaczorowski, T.; Prochowicz, D.; Lipińska, T.; Justyniak, I.; Kaszkur, Z.; Lipkowski, J. *Angew. Chem., Int. Ed.* **2010**, *49*, 7035–7039.